

Synthesis and third order nonlinear optics of a new soluble conjugated porphyrin polymer†

Thomas E. O. Screen,^a Katrina B. Lawton,^a G. Scott Wilson,^a Nicole Dolney,^b Radu Ispasoiu,^b Theodore Goodson III,^b Simon J. Martin,^c Donal D. C. Bradley^{c‡} and Harry L. Anderson^{*a}

^aDepartment of Chemistry, University of Oxford, Dyson Perrins Laboratory, South Parks Road, Oxford, UK OX1 3QY. E-mail: harry.anderson@chem.ox.ac.uk

^bDepartment of Chemistry, Wayne State University, Detroit, USA MI 48202

^cDepartment of Physics, University of Sheffield, Hick's Building, Hounsfield Road, Sheffield, UK S3 7HR

Received 7th September 2000, Accepted 30th October 2000

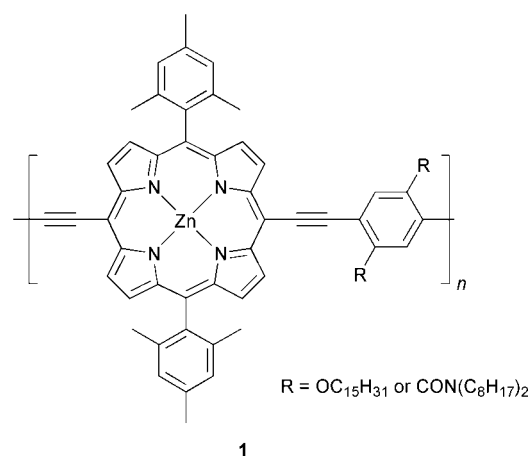
First published as an Advance Article on the web 2nd January 2001

The synthesis of a new soluble conjugated porphyrin polymer **4** is reported. The MALDI TOF mass spectrum shows the presence of oligomers with up to 13 repeat units and GPC gives a M_n of 53 kDa. The electronic absorption spectra of this polymer exhibit an intense Q band at 800 nm in solution and 853 nm in the solid state, demonstrating a high degree of conjugation. Electroabsorption spectroscopy shows that thin films of **4** have lower resonant third order NLO susceptibility than our previous conjugated porphyrin polymer **2**, whereas closed z -scan measurements indicate that the off-resonance real susceptibility, at 1064 nm, is exceptionally large for both polymers ($\chi_R^{(3)} = -2 \times 10^{-16} \text{ m}^2 \text{ V}^{-2}$). Open z -scan measurements were also made at 1064 nm, demonstrating that the two polymers exhibit similar nonlinear absorption at this wavelength ($\beta = 1 \text{ cm GW}^{-1}$ at 0.2 mM concentration).

Introduction

Simple conjugated polymers such as poly(*p*-phenylene) and poly(*p*-phenylenevinylene) exhibit useful properties, including semiconductivity and electroluminescence.¹ Recently, interest in advanced electronic and photonic materials has led to the exploration of conjugated polymers of more complex units, such as porphyrins.² The high polarisability and optical oscillator strength of the porphyrin macrocycles gives these materials remarkable nonlinear optical (NLO) behaviour, making them potentially useful for ultra-fast switching technologies. High values of the nonlinear refractive index, n_2 (which is proportional to the real part of the third order susceptibility, $\chi^{(3)}$) are essential for electro-optical and all-optical switching,³ whereas high nonlinear absorption coefficients, β (proportional to the imaginary part of $\chi^{(3)}$) are important for optical limiting.⁴ High values of $\chi^{(3)}$ are associated with large, polarisable π -systems, long conjugation lengths and small HOMO–LUMO gaps,⁵ which explains why porphyrins are good building blocks for such materials. The possibilities of substitution around the porphyrin periphery and of varying the metal at the centre of the porphyrin provide extra ways of optimising the performance of these material.

The syntheses of several conjugated porphyrin polymers have been reported. The aryl acetylene linked polymer **1**, was prepared by Jones *et al.*, by palladium catalysed Heck–Sonogashira coupling of the 5,15-diethynyl porphyrin with 1,4-diiodophenylenes.⁶ GPC of this material gave molecular weights of $M_w = 52000$ and $M_n = 25000$ (relative to polystyrene standards). Therien and DiMugno briefly reported the



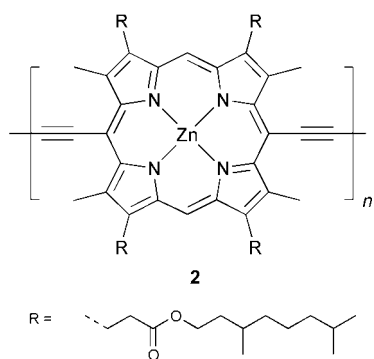
syntheses of various porphyrin polymers, including a poly-(diethynylaryl porphyrin) in a patent.⁷

The butadiyne link provides an attractive route to conjugated porphyrin oligomers and polymers. Glaser–Hay coupling⁸ of terminal acetylenes has been used to form long conjugated polymers from simple aromatic organic monomers.⁹ Soluble conjugated porphyrin polymer **2** has been prepared by this route.¹⁰ This polymer has an exceptionally high value of $\chi^{(3)}$ and is very soluble in chlorinated solvents in the presence of a ligand such as pyridine which coordinates to the zinc.¹¹

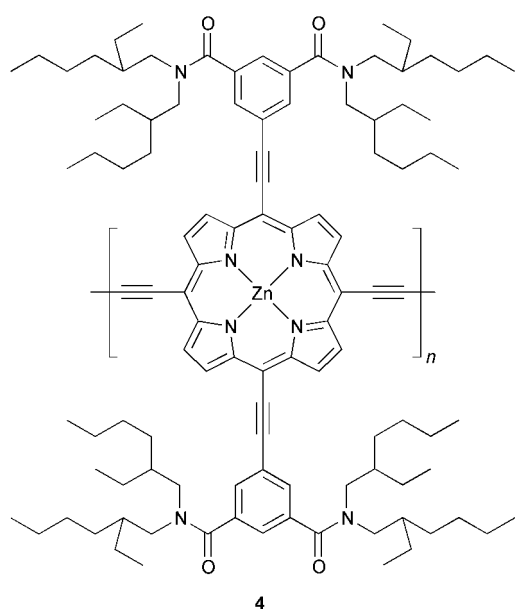
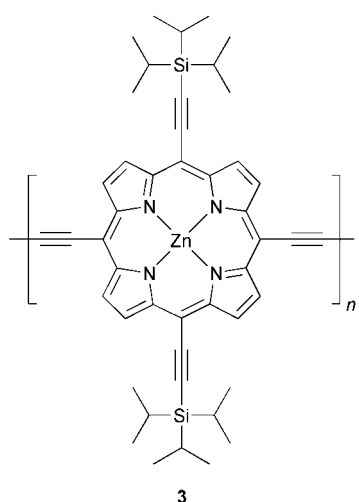
Here we report an investigation of *meso-meso* butadiyne-linked porphyrin polymers with alkyne substituents on the *meso* positions perpendicular to the polymer backbone. We hoped that this design would increase the electronic delocalisation, by allowing conjugation in two dimensions, and result in sharper absorption, by maintaining a local D_{4h} symmetry for each chromophore. The attachment of solubilising groups to these *meso*-ethynyl substituents (as opposed to *meso*-aryls)

†Spectroscopic and analytical data for compounds prepared in this paper are available as supplementary data. For direct electronic access see <http://www.rsc.org/suppdata/jm/b0/b007250h/>

‡Current address: Department of Physics, Imperial College, London UK SW7 2BZ.



should allow the whole molecule to be planar, encouraging ordered stacking in the solid state, which could increase the conjugation and the sharpness of absorption. In order to be useful for optoelectronic applications, polymers need to be soluble enough for thin film fabrication by spin coating from solution. Simple porphyrins tend to have low solubility, so choice of solubilising groups is a crucial aspect in the design of any rigid-rod conjugated porphyrin polymer. In this work, our initial target was the triisopropylsilyl substituted polymer **3**, but this material turned out to be insoluble, so we redesigned the synthesis to gain access to a new soluble conjugated porphyrin polymer **4**. We found that the electronic spectra of **4** are broader than those of **2**, but the two materials appear to



have similar NLO characteristics in the near infrared at 1064 nm.

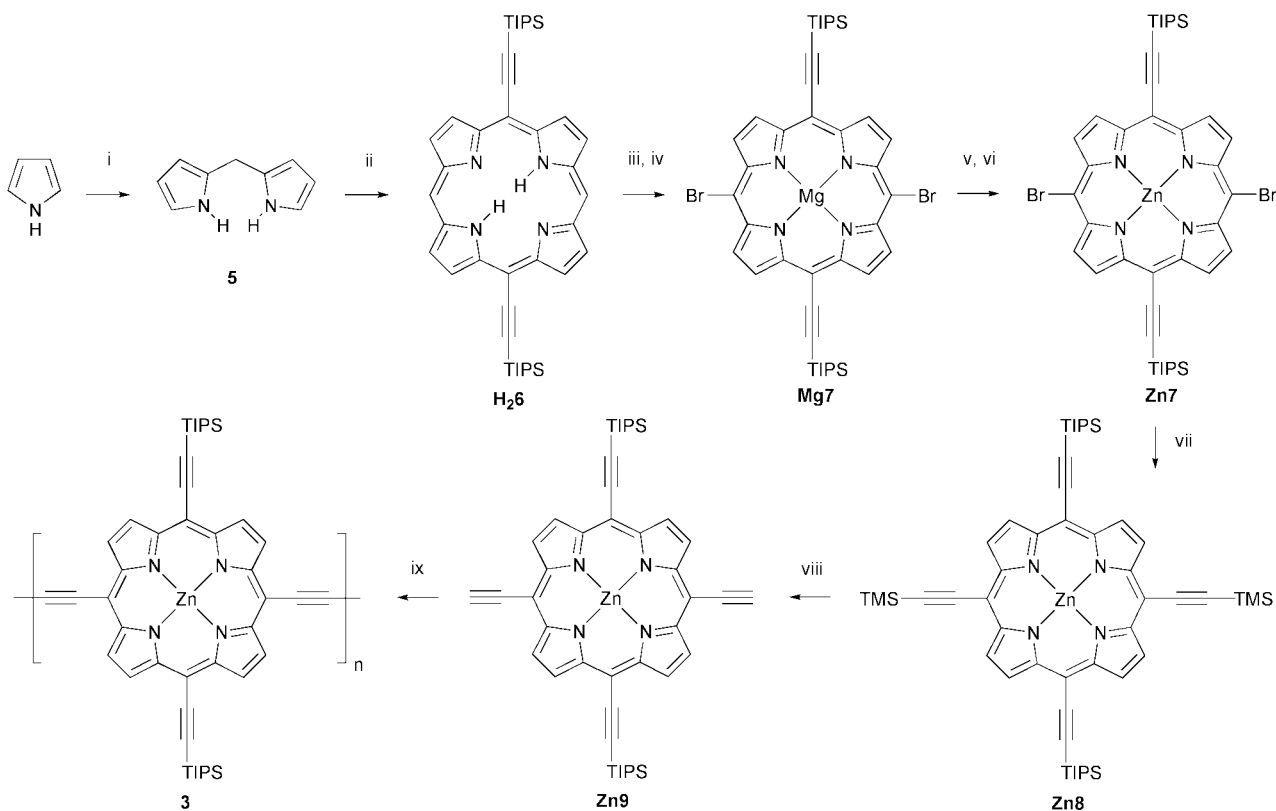
Results and discussion

Synthesis

We initially sought to prepare conjugated porphyrin polymer **3** using the synthetic route summarised in Scheme 1 (part of this synthesis has been reported in a preliminary communication¹²). The starting material, dipyrromethane **5**, was prepared by passing formaldehyde gas into pyrrole containing trifluoroacetic acid. We find that on a multi-gram scale this method gives higher yields than Wang and Bruce's procedure, which uses paraformaldehyde.¹³ Our route is also more direct than the commonly used route of Clezy *et al.*¹⁴ Recently Lindsey and co-workers have reported another procedure for preparing **5** directly from paraformaldehyde.¹⁵ Condensation of **5** with triisopropylsilylpropynal¹⁶ using boron trifluoride, followed by DDQ oxidation gave the porphyrin **H26** in 29% yield.¹⁷ Next we sought to brominate this porphyrin at the two free *meso*-positions, to activate it for coupling to two more alkyne substituents. Direct bromination of the free-base, and of the zinc complex **Zn6**, were unsatisfactory, with significant amounts of reaction at the β -positions and on the alkynes. The electron withdrawing 5,15-dialkynyl substituents evidently make **6** much less reactive than a 5,15-diaryl porphyrin. This problem was overcome by using the more electron-rich magnesium porphyrin **Mg6**, which reacts cleanly at the *meso* positions to give **Mg7**.¹⁸ Demetallation with TFA and reaction with zinc acetate were used to form the zinc complex **Zn7**. A range of reaction conditions were tested for the Heck–Sonogashira coupling of **Zn7** with trimethylsilyl acetylene. Initially we tried to avoid using copper(I) iodide co-catalyst, because we were concerned that copper might insert into the porphyrin,¹⁹ but we were unable to achieve efficient coupling in the absence of CuI, even when using the zinc acetylide TMSC_2ZnCl .²⁰ In fact metallation and demetallation of *meso*-ethynyl porphyrins is much slower than that of *meso*-aryl porphyrins and transmetallation is not a problem. Coupling was found to reach completion in about 3 hours at 80 °C using three equivalents of trimethylsilylacetylene, 10 mol% palladium and 20 mol% CuI in toluene–triethylamine–pyridine.²¹ This coupling reaction was also attempted on **Mg7**, to give **Mg8**, but we found that the reaction worked less efficiently with the magnesium complex, as would be expected, since electron-rich aryl halides tend to be less reactive towards Heck–Sonogashira coupling.

Having gained access to the differentially protected *meso*-tetraethynyl porphyrin **Zn8**, we selectively deprotected the trimethylsilylalkyne with methanolic potassium carbonate,²² to give our bis-functional monomer **Zn9**. Polymerisation of this material under Glaser–Hay conditions¹⁰ gave a material which we assume to be **3**, however this polymer is insoluble in solvents such as chloroform, even in the presence of pyridine and quinuclidine, which precluded spectroscopic characterisation.

This forced us to redesign the target structure, to incorporate larger solubilising side chains, leading to the choice of polymer **4** as a new target, with branched racemic 2-ethylhexyl substituents. The aryl rings in **4** can lie co-planar with the porphyrin, due to the alkyne spacers, further extending the conjugation. The solubilising group **13** was synthesised in high yield from 5-iodoisophthalic acid using established methodology,²³ as shown in Scheme 2. This alkyne was then attached to dibromoporphyrin **Zn7** using Heck–Sonogashira coupling to give the highly soluble protected monomer **Zn14** (Scheme 3). Use of a pre-formed Pd/Cu catalyst solution²⁴ enabled us to achieve this coupling in 95% yield. We found it practical to use samples of impure **Zn7** containing some mono-bromo porphyrin in this reaction, because the impurity becomes



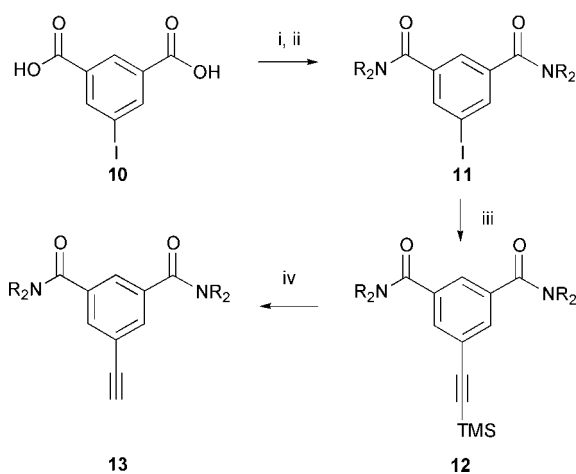
Scheme 1 Synthetic route to polymer 3. *Reagents, conditions and yields:* i, CH₂O, TFA, 63%; ii, TIPSC₂CHO, BF₃·OEt₂ then DDQ, 29%; iii, MgI₂, Et₃N, pyridine, 97%; iv, NBS, 75%; v, TFA, 94%; vi, Zn(OAc)₂, 84%; vii, TMSC₂H, Pd₂dba₃, PPh₃, CuI; viii, K₂CO₃, MeOH, 66% over two steps; ix, CuCl, TMEDA, O₂, 43%.

much easier to remove after coupling to the solubilising side chains. Removal of the TIPS protecting groups with TBAF to give monomer **Zn15**, followed by Glaser-Hay coupling gave the target polymer **4** in 71% yield.

A dimeric analogue of **4** was also prepared to provide a model compound for comparison with the polymer (Scheme 4). Mono-protected compound **Zn16** was obtained from partial deprotection of **Zn14**. Glaser coupling of this material gave the dimer **Zn17** in 87% yield.

Polymer characterisation

Polymer **4** is very soluble in organic solvents in the presence of coordinating ligands. Concentrations of less than 1% pyridine give good solubility in a range of solvents. Once all the pyridine

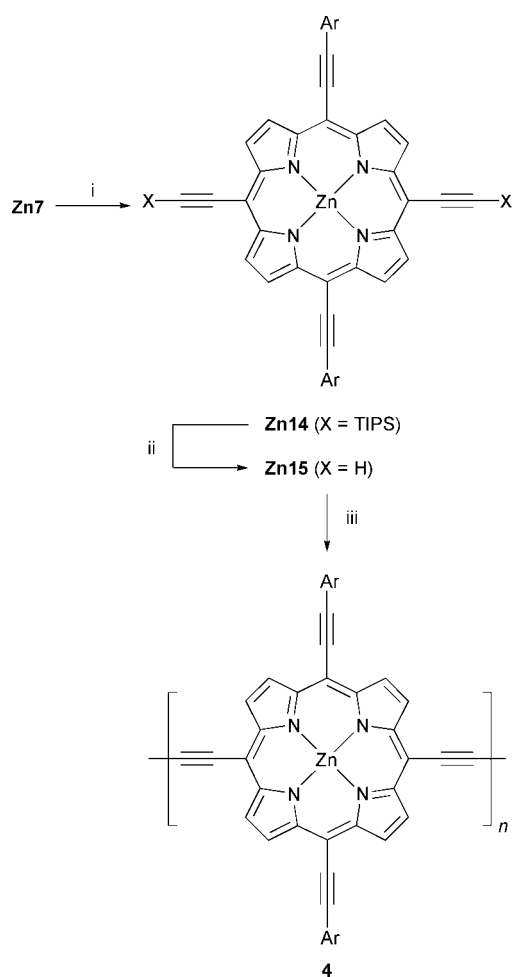


Scheme 2 Synthesis of the solubilising alkyne **13** (R = CH₂CHEtCH₂CH₂CH₂CH₃). *Reagents, conditions and yields:* i, SOCl₂; ii, HNR₂, Et₃N, PhMe, 99% over two steps; iii, TMSC₂H, Pd(OAc)₂, PPh₃, CuI, Et₃N, 89%; iv, K₂CO₃, MeOH, 94%.

has been removed from the polymer (by precipitating with methanol and vacuum drying), a hard, black-green material is obtained. This is slightly soluble in chloroform and dichloromethane, soluble in THF, and very slightly soluble in toluene; it is insoluble in hexane, ethyl acetate and methanol.

The ¹H and ¹³C NMR spectra of polymer **4** are consistent with the proposed structure. No signals for terminal acetylenes are detected by ¹H NMR or IR. The expected number of ¹³C resonances are observed, although the signals due to the acetylene and porphyrin carbons in the polymer backbone are very broad, as found previously with polymer **2**. The ethylhexyl signals are split, due the presence of two non-equivalent ethylhexyl groups on the amide, and due to the racemic nature of this solubilising group. IR spectra (in KBr) show two weak C≡C stretch signals at 2177 and 2121 cm⁻¹ for the acetylenes in the polymer backbone and between the porphyrin and aryl groups. The UV-Vis spectrum of the polymer displays a large red-shift, and intensification, of the Q-band and a broadening of the Soret band, associated with strong electronic communication between the porphyrins. The absorption spectra of the monomer **Zn15**, dimer **Zn17** and polymer **4** in 1% pyridine-dichloromethane (Fig. 1) have Q-band λ_{max} of 671, 693 and 800 nm respectively. Comparison of the absorption spectra of polymers **4** and **2**, in 1% pyridine-dichloromethane (Fig. 2) shows that the original polymer **2** has a sharper and more red-shifted Q-band. Under the same conditions, polymers **4** and **2** exhibit fluorescence emission bands at 824 and 860 nm respectively, confirming that **2** has a smaller HOMO-LUMO gap. However in the solid state the absorption of **4** shifts to longer wavelength than that of **2** (Fig. 3). Good optical quality thin films of both polymers were spin cast from CHCl₃-pyridine solutions. The sharper more red-shifted Q-band of **4** in the solid state is probably due to the adoption of more ordered planar conformations, with less torsional disorder.

The solubility of the polymers in THF allowed elucidation of chain length by GPC. Polymer **4** was run in THF and



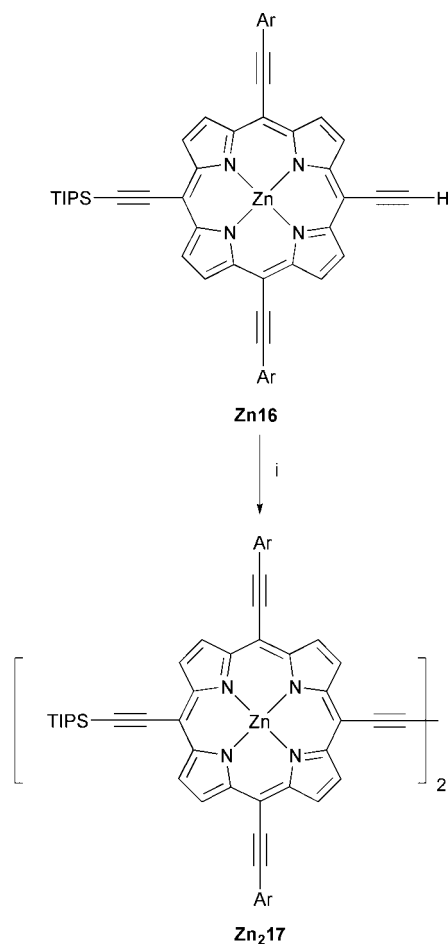
Scheme 3 Synthetic route to polymer **4**. Reagents, conditions and yields: i, **13**, Pd₂dba₃, PPh₃, CuI, 95%; ii, TBAF, 89%; iii, CuCl, TMEDA, O₂, 71%.

compared to polystyrene standards giving molecular weight averages of $M_w = 119\,000$ and $M_n = 53\,000$. GPC on polymer **2** under identical conditions gave values of $M_w = 55\,000$ and $M_n = 40\,000$. This corresponds to an average of around 30 repeat units in both polymers, and implies that they have higher molecular weights than polymer **1**.⁶ These results gain some support from MALDI-TOF mass spectrometry on **4**. Peaks are found extending to 23 000 Da, corresponding to around 13 repeat units (Fig. 4). Unfortunately the resolution is too low to elucidate the end groups. All attempts to obtain a MALDI TOF mass spectrum of polymer **2** were unsuccessful. The molecular weight of **2** from GPC is significantly higher than that previously deduced from small angle neutron scattering (7–15 repeat units).¹⁰

Nonlinear optics

The third order nonlinear optical susceptibility and optical limiting properties of polymer **4** were compared with those of the previously reported polymer **2** using electroabsorption spectroscopy and *z*-scan measurements.

Electroabsorption spectroscopy is a useful technique for investigating electronic transitions and determining the quadratic electro-optic susceptibility $\chi^{(3)}(-\omega; 0, 0, \omega)$ by measuring the change in absorbance of a sample in response to a sinusoidal electric field.^{25–27} Measurements on a 670 Å thick spun film of the polymer showed an electroabsorption response proportional to the square of the electric field strength, as expected for a third order NLO material. The shape of the electroabsorption curve matches closely to that of the first derivative of absorption, suggesting absorption results in



Scheme 4 Synthesis of the dimer model compound **Zn₂17**. Reagents, conditions and yields: i, CuCl, TMEDA, O₂, 87%.

neutral localised excitons, as found with polymer **2**.¹⁰ The real and imaginary components of $\chi^{(3)}(-\omega; 0, 0, \omega)$ were calculated from the electroabsorption spectrum²⁵ and are shown in Fig. 5. The polymer **4** gives a real peak resonant $\chi^{(3)}_R$ of $7 \times 10^{-17} \text{ m}^2 \text{ V}^{-2}$. This is significantly lower than the value of $1.0 \times 10^{-15} \text{ m}^2 \text{ V}^{-2}$ for polymer **2**¹⁰ previously obtained by the same technique. However the resonant nonlinearity, at the centre of the Q-band, is less relevant to potential switching applications than the nonlinearity at longer wavelengths, in the fibre-optics telecommunications window, where these polymers are transparent. Previously degenerate four wave mixing (DFWM) experiments have shown that polymer **2** exhibits an off-resonant $\chi^{(3)}$ at 1064 nm which is higher than that reported for any other organic material.¹¹ In this study we

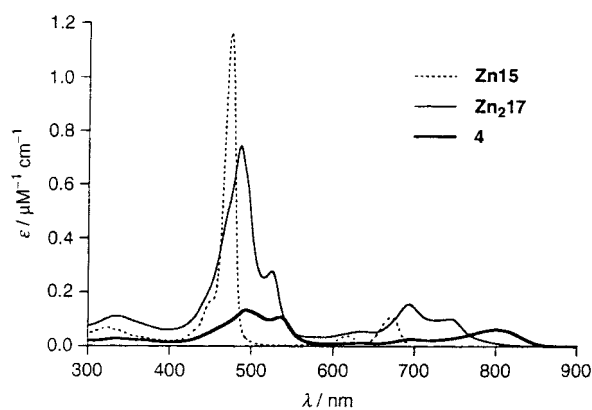


Fig. 1 Absorption spectra of the monomer **Zn15**, dimer **Zn₂17** and polymer **4** in 1% pyridine-dichloromethane (extinction coefficients for **4** are per repeat unit).

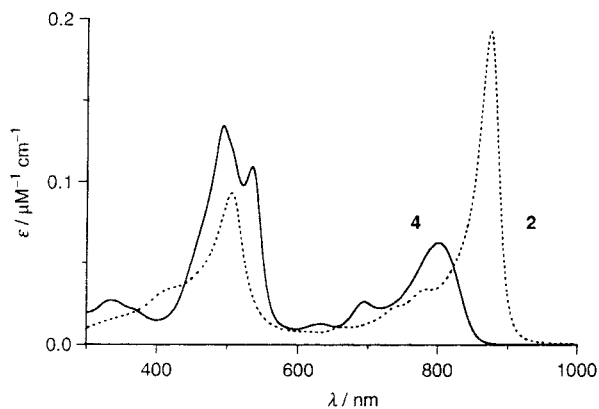


Fig. 2 Absorption spectra of **4** (solid line) and **2** (dashed) in 1% pyridine–dichloromethane (absorption coefficients are per repeat unit).

compared the third order nonlinearities of **4** and **2** at 1064 nm using *z*-scan measurements.²⁸

The basic principle of the closed-aperture *z*-scan experiment²⁹ is that the sample is moved through the focus of a laser beam, and the intensity transmitted through a small aperture, immediately in front of the detector, is measured. The sample acts as a nonlinear lens, distorting the wavefront of the light beam and changing the amount of light passing through the aperture as the *z*-position is altered (*z*=0 at the focus). The *z*-position/transmission dependence allows the calculation of the nonlinear refraction, which is related to nonlinear susceptibility. The closed *z*-scan results for polymer **4** and polymer **2** (as solutions in 1% pyridine–chloroform) are compared in Figs 6a and 6b. The strong nonlinear refraction produces a peak–valley curve, with a pre-focal maximum followed by a post-focal minimum, which demonstrates a nonlinear refractive index, n_2 , with a negative sign. The symmetrical shape of these plots shows that nonlinear refraction effects dominate any nonlinear absorption, which makes it simple to calculate the value of n_2 from the difference between the normalised peak and valley transmissions. This gave values of n_2 of $-1.6 \times 10^{-5} \text{ cm}^2 \text{ GW}^{-1}$ and $-7.8 \times 10^{-5} \text{ cm}^2 \text{ GW}^{-1}$ for solutions of **4** and **2** respectively. The real third order susceptibility $\chi^{(3)}_{\text{R}}$ was calculated from the nonlinear refractive index n_2 using eqn. (1), where ϵ_0 is the vacuum permittivity, c is the speed of light and n_0 is the linear refractive index.³⁰

$$\chi^{(3)}_{\text{R}} = (4/3)\epsilon_0 c n_0 n_2 \quad (1)$$

This gave $\chi^{(3)}_{\text{R}} = -1.2 \times 10^{-20} \text{ m}^2 \text{ V}^{-2}$ and $-5.8 \times 10^{-20} \text{ m}^2 \text{ V}^{-2}$ for solutions of polymers **4** and **2**, at concentrations of $4.2 \times 10^{-5} \text{ M}$ and $2.2 \times 10^{-4} \text{ M}$ respectively. Assuming that the $\chi^{(3)}$ of each solution is proportional to the volume fraction of the porphyrin polymer, this corresponds to bulk

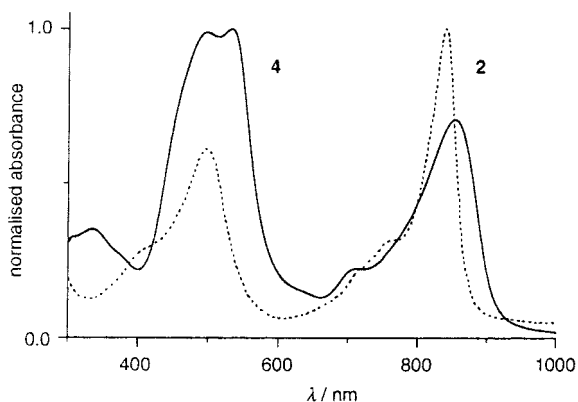


Fig. 3 Solid state absorption spectra of polymers **4** (solid line) and **2** (dashed line) spin coated on glass.

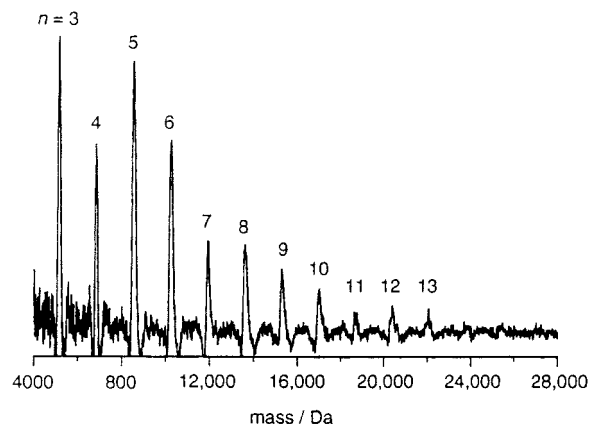


Fig. 4 MALDI-TOF mass spectrum of **4**, from a dithranol matrix.

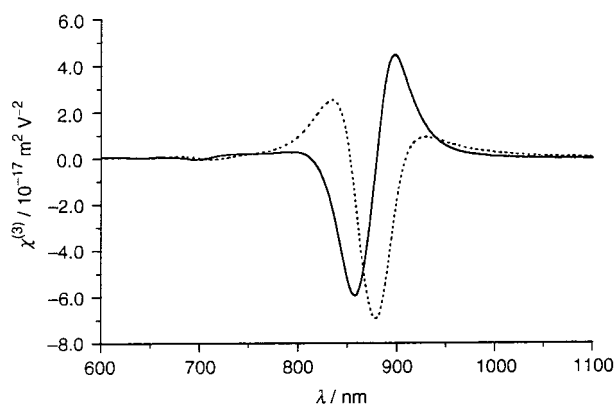


Fig. 5 Real (solid) and imaginary (dashed) $\chi^{(3)}(-\omega;0,0,\omega)$ spectra of **4** from electroabsorption spectroscopy on a thin film of the pure polymer.

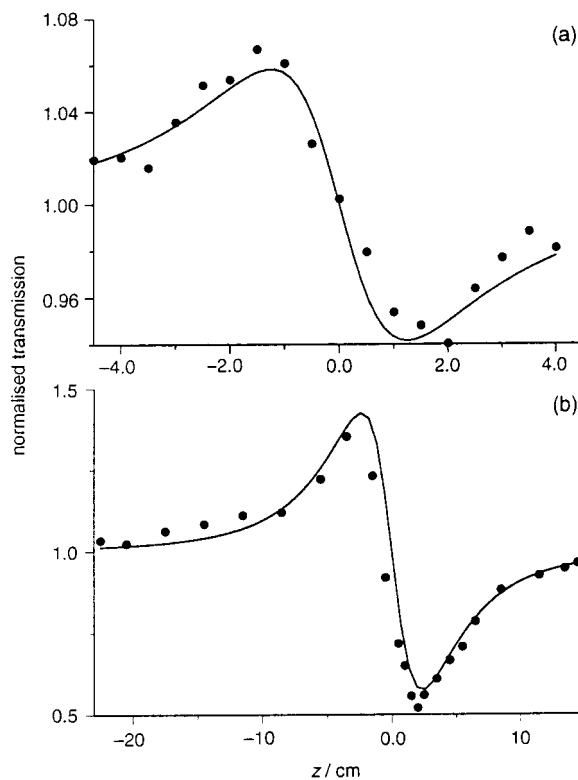


Fig. 6 Closed *z*-scan measurement on (a) **4** (conc. = 0.04 mM; $\lambda = 1064 \text{ nm}$; $I_0 = 0.32 \text{ GW cm}^{-2}$; $f = 10 \text{ cm}$; $n_2 = 1.6 \times 10^{-5} \text{ cm}^2 \text{ GW}^{-1}$) and (b) **2** (conc. = 0.2 mM; $\lambda = 1064 \text{ nm}$; $I_0 = 0.50 \text{ GW cm}^{-2}$; $f = 35 \text{ cm}$; $n_2 = 7.8 \times 10^{-5} \text{ cm}^2 \text{ GW}^{-1}$).

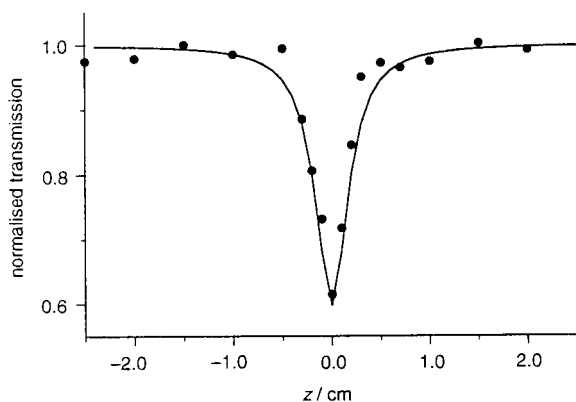


Fig. 7 Open z -scan measurements on (a) **4** (conc.=0.2 mM; $\lambda=1064$ nm; $I_0=1.5$ GW cm $^{-2}$; $f=10$ cm; spot radius=0.03 mm; $\beta=1.1$ cm GW $^{-1}$).

susceptibilities of $\chi^{(3)}_{\text{R}}=-1.7 \times 10^{-16}$ m 2 V $^{-2}$ for **4** and $\chi^{(3)}_{\text{R}}=-1.9 \times 10^{-16}$ m 2 V $^{-2}$ for **2**. This value for **2** compares well with the previous measurements by DFWM, at the same wavelength ($\chi^{(3)}_{\text{xyyx}}=-2.9 \times 10^{-17}$ m 2 V $^{-2}$), for the bulk material.¹¹ Thus our closed z -scan measurements indicate that polymers **4** and **2** have similar NLO behaviour at 1064 nm. The observation of a one-photon off-resonant $\chi^{(3)}(-\omega-\omega,\omega,\omega)$ for **4** from z -scan measurements which is larger than the peak resonant $\chi^{(3)}(-\omega;0,0,\omega)$ from electroabsorption implies that the z -scan response is enhanced by some two-photon resonance with the Soret band, or by other contributions such as reorientation effects.

Open-aperture z -scan measurements were also used to test for nonlinear absorption at 1064 nm. This experiment is similar to that for the closed z -scans, except that now all the light passing through the sample is collected by the detector, so that refraction effects are not observed. The open z -scan traces for both polymers were fitted to a two-photon absorption giving $\beta=1.0$ cm GW $^{-1}$ for **2** and $\beta=1.1$ cm GW $^{-1}$ for **4**; for example the curve for polymer **4** is shown in Fig. 7.

Conclusions

We have described the synthesis of a new soluble butadiyne-linked conjugated porphyrin polymer **4** which has ethynylaryl substituents extending the conjugation of the porphyrin perpendicular to the main chain. GPC shows that this polymer has an average of about 30 repeat units, and oligomers with up to 15 repeat units are detected by MALDI TOF MS. The absorption and emission spectra of polymer **4** show that it has a similar HOMO-LUMO gap to our previous conjugated porphyrin polymer **2**. The resonant nonlinear susceptibilities $\chi^{(3)}$ of both polymers were compared using electroabsorption spectroscopy; **4** has a lower resonant real $\chi^{(3)}$ than **2**, perhaps because of its broader absorption. However at 1064 nm, where there is minimal absorption, closed z -scan measurements indicate that both polymers have non-resonant $\chi^{(3)}$ values of about 2×10^{-16} m 2 V $^{-2}$. This agrees with previous measurements on **2** by DFWM at the same wavelength. The optical limiting behaviour of both polymers have been explored using the open z -scan technique, which gave two-photon absorption coefficients of $\beta=1$ cm GW $^{-1}$ for both compounds at 0.2 mM concentration. The extended two-dimensional conjugation in **4**, compared to **2**, does not seem to result in increased optical nonlinearity. While this is disappointing, it fits in with the observation that 1D π -systems generally have higher nonlinearities per π -electron than 2D π -systems.³¹ The main advantages of our new polymer **4** are its easier synthesis and higher solubility. The observation of a strong nonlinear refraction at 1064 nm is encouraging for the use of these materials in all-optical or electro-optical switching applica-

tions. These materials may also be appropriate for optical squeezing, where both large $\chi^{(3)}$ and large β values can be utilised.³²

Experimental

General

All manipulations of air- and water-sensitive compounds were performed using standard high-vacuum or Schlenk line techniques. THF was distilled from sodium-benzophenone under nitrogen prior to use. Dichloromethane and toluene were distilled from CaH $_2$ under nitrogen prior to use. All other reagents were used as commercially supplied. NMR spectra were recorded at ambient probe temperature, unless otherwise stated, using Bruker AM500 (500 MHz) and Varian Gemini 200 (200 MHz) instruments. Coupling constants (J) are given in Hz. IR spectra were recorded using a Perkin Elmer 1750 FT-IR spectrometer. UV-vis-near IR absorption spectra were recorded on a Perkin Elmer Lambda 20 spectrometer. Fluorescence emission spectra were recorded on a Spex FluoroMax-2 fluorimeter with a red-sensitive R2658-P photomultiplier tube. Mass spectra were carried out using atmospheric pressure chemical ionisation (APCI), fast atom bombardment (FAB) by the EPSRC Mass Spectrometry Service in Swansea, and MALDI TOF on a Micromass ToF Spec 2E. Only molecular ions and major peaks are reported. Analytical gel permeation chromatography was carried out with a Polymer Laboratories Plgel 20 μ m MIXED-A column calibrated with polystyrene narrow standards (MW 580–11.6 $\times 10^6$) in THF with toluene as a flow marker; the flow rate was 1 cm 3 min $^{-1}$ at 30 $^\circ$ C and the UV detector was set to 257 nm. Flash column chromatography was carried out on silica gel 60 GF $_{254}$. Analytical TLC was carried out on Merck[®] aluminium backed silica gel 60 F $_{254}$ plates. Uncorrected melting points were measured on a Gallenkamp capillary melting point apparatus. Spectroscopic and analytical data for compounds prepared here are available as supplementary information.†

Electroabsorption spectroscopy

Samples for electroabsorption measurements were made by spin coating a thin film of **4** onto a spectroil B disk. An aluminium interdigitated electrode array, with finger spacing 100 μ m, was then deposited on top of the film by thermal evaporation of the aluminium through a mask under high vacuum. The sample was then mounted in the electroabsorption spectrometer. For all measurements the sample was kept under dynamic vacuum ($<10^{-5}$ Torr). A sinusoidally varying voltage in the range 300 to 700 V (frequency 2 kHz) was then applied to the sample. The optical transmission, T , and the electric field induced change in the transmission ΔT were recorded in the wavelength range 1100 to 600 nm. The normalised change in transmission ($\Delta T/T$) was calculated, which could then be used to calculate the real and imaginary parts of $\chi^{(3)}(-\omega;0,0,\omega)$ via a Kramers-Kronig analysis.

z -Scan measurements

Solutions for z -scan measurements were made up in 1% pyridine-chloroform and passed through a 0.2 μ m filter before being placed in a 1.0 cm optical path length cell. The light source was a Nd:YAG laser ($\lambda=1064$ nm) with a pulse duration of 6 ns and a repetition rate of 100 Hz. Open aperture z -scans were performed by collecting the transmitted beam with a large area power meter and closed z -scans were performed by inserting a small aperture (0.5 mm diameter) in the far-field. The beam intensity I_0 and the focal length of the lens f are indicated in the captions to Figs. 6 and 7. Negative values of z correspond to sample positions before the focal point of the

beam. The details of the *z*-scan experiment have been reported previously.²⁸

Dipyrrromethane (5)

Formaldehyde gas was generated by cracking paraformaldehyde (1.35 g, 45 mmol) at 170 °C for 15 min, and passed into an oxygen-free solution of TFA (347 μ l, 4.5 mmol) in pyrrole (250 ml, 3.6 mol) under a slow flow of argon. The reaction mixture was stirred at room temperature for 15 min after all the paraformaldehyde had been transferred, then the yellow solution was diluted with CH₂Cl₂ (100 ml), and washed with water (3 \times 200 ml), then NaOH (aq, 0.1 M, 2 \times 200 ml), then water (2 \times 200 ml), then evaporated and dried under vacuum. Column chromatography (60–80 petroleum ether–EtOAc–Et₃N 10:1:0.1) was used to isolate the product. Fractions containing dipyrrromethane were evaporated and vacuum dried to yield **5** (4.15 g, 63%).

Triisopropylsilylpropynal

Previously this compound has been prepared by oxidation of the alcohol.¹⁶ We made it from TIPS-acetylene using the following procedure: *n*-Butyllithium (44 ml, 1.6 M in hexanes, 71 mmol) was added dropwise to a solution of triisopropylsilylacetylene (15 ml, 67.5 mmol) in THF (150 ml) at 0 °C. The mixture was stirred at 0 °C for 20 min, then at room temperature for 20 min, then re-cooled to 0 °C and DMF (4.9 ml, 71 mmol) was added slowly with stirring. The mixture was allowed to warm to room temperature over 20 min, then heated to reflux for 1 h, before cooling to 0 °C and treating with sulfuric acid (5% aq., 120 ml). NaHCO₃ aq. was added until the mixture was at pH 5, then the product was extracted with CH₂Cl₂ (4 \times 50 ml) and washed with water (100 ml). Evaporation of the solvent and vacuum distillation, collecting the fraction 40–45 °C/0.15 mmHg, yielded the product as a colourless oil (12.16 g, 86%).

5,15-Bis[(triisopropylsilyl)ethynyl]porphyrin (H₂6)

BF₃·Et₂O (278 μ l, 2.19 mmol) was added to an oxygen-free solution of dipyrrromethane **5** (0.987 g, 6.75 mmol) and triisopropylsilylpropynal (1.52 ml, 6.76 mmol) in CH₂Cl₂ (400 ml). The mixture was stirred for 45 min, over which time it turned dark blue. DDQ (2.30 g, 10.1 mmol) was then added and the mixture stirred for 10 min. The resulting brown solution was filtered through silica gel with CH₂Cl₂ as the eluent, to remove DDQ residues and tar, then concentrated and chromatographed on silica gel (CH₂Cl₂). After solvent removal, **H₂6** was recrystallised from CH₂Cl₂–methanol in 0.65 g (29%) yield.

{5,15-Bis[(triisopropylsilyl)ethynyl]porphyrinato}magnesium(II) (Mg6)

A solution of the free-base porphyrin **H₂6** (0.500 g, 0.75 mmol) and MgI₂ (0.834 g, 3.00 mmol) in pyridine (35 ml) and Et₃N (1.5 ml) was refluxed for 24 h, under argon, during which time the mixture became bright green. The pyridine was distilled off at ambient pressure, and the residue redissolved in CH₂Cl₂ and chromatographed (CH₂Cl₂–5% Et₃N as eluent). Solvent evaporation and recrystallisation from CH₂Cl₂ by layered addition of methanol, and methanol–10% water afforded dark green crystals of **Mg6** (0.501 g, 97%).

{5,15-Dibromo-10,20-bis[(triisopropylsilyl)ethynyl]porphyrinato}magnesium(II) (Mg7)

NBS (0.191 g, 1.07 mmol) was added to a stirred solution of **Mg6** (0.354 g, 0.511 mmol) in CHCl₃ (45 ml) and pyridine (0.45 ml). The reaction was monitored by TLC (60–80 petroleum ether–EtOAc–pyridine 10:1:0.1) and quenched

by the addition of acetone (20 ml) after 15 min. The crude reaction mixture was evaporated and chromatographed, eluting with the same solvent system as TLC. Fractions containing the slower running tribrominated products were discarded, while those containing the di-bromo product were evaporated and dried under vacuum to yield **Mg7** (0.325 g, 75%).

5,15-Dibromo-10,20-bis[(triisopropylsilyl)ethynyl]porphyrin (H₂7)

A solution of **Mg7** (0.325 g, 0.38 mmol) in CHCl₃ (28 ml) was treated with TFA (0.147 ml, 1.91 mmol). The reaction was monitored by TLC (60–80 petroleum ether–EtOAc–pyridine 10:1:0.1). Once complete (approx. 5 min) the solution was washed with water, evaporated and filtered through silica (CH₂Cl₂–60–80 petroleum ether 3:1 as eluent). Recrystallisation from CH₂Cl₂–methanol yielded the free-base porphyrin **H₂7** (0.238 g, 94%).

{5,15-Dibromo-10,20-bis[(triisopropylsilyl)ethynyl]porphyrinato}zinc(II) (Zn7)

A solution of **H₂7** (0.238 g, 0.288 mmol) in CHCl₃ (28 ml) was refluxed with Zn(OAc)₂·2H₂O (0.316 g, 1.44 mmol) in methanol (2.5 ml) for 2 h. When TLC (60–80 petroleum ether–CH₂Cl₂ 2:1) confirmed completion, the solution was concentrated and filtered through silica with chloroform as eluent. Recrystallisation from CH₂Cl₂–methanol yielded **Zn7** as a green solid (0.216 g, 84%).

{5,15-Diethynyl-10,20-bis[(triisopropylsilyl)ethynyl]porphyrinato}zinc(II) (Zn9)

Trimethylsilylacetylene (96 μ l, 0.67 mmol) was added to a solution of **Zn7** (0.200 g, 0.224 mmol), Pd₂(dba)₃ (12.5 mg, 0.014 mmol), PPh₃ (29 mg, 0.11 mmol) and CuI (11 mg, 0.056 mmol) in toluene (65 ml), Et₃N (14 ml) and pyridine (800 μ l) under argon, and the mixture was heated to 80 °C for 3 h. The mixture was washed with water (2 \times 100 ml), evaporated and chromatographed (60–80 petroleum ether–CH₂Cl₂ 3:1 gradually increased to 60–80 petroleum ether–CH₂Cl₂ 1:1 as eluent). After solvent removal, the intermediate (**Zn8**) was dried under high vacuum and a proton NMR spectrum recorded, before proceeding to deprotection. δ_{H} (200 MHz, CDCl₃) 9.62 (8 H, AB quartet, β H), 1.49–1.47 (42 H, m, TIPS*H*), 0.64 (18 H, s, TMS *H*); *R*_f=0.35 (60–80 petroleum ether–CH₂Cl₂ 2:1). The crude **Zn8** was dissolved in THF (185 ml) and treated with K₂CO₃ (0.21 g, 1.5 mmol) and methanol (56 ml). After vigorously stirring for 30 min, the reaction mixture was partitioned between toluene (100 ml) and water (100 ml). The organic layer was separated, washed with water (2 \times 100 ml) and evaporated. Recrystallisation from toluene–30–40 petroleum ether, yielded the product **Zn9** (0.116 g, 66% over 2 steps).

N,N,N',N'-Tetrakis(2-ethylhexyl)-5-iodoisophthalamide (11)

5-Iodoisophthalic acid **10** (3.0 g, 10.4 mmol) was refluxed in SOCl₂ (40 ml) for 16 h. Excess SOCl₂ was removed by distillation at ambient pressure, followed by vacuum drying, to leave the acid chloride intermediate as a pale brown oil. ν_{max} (NaCl)/cm⁻¹ 1759 (C=O); δ_{H} (200 MHz; CDCl₃) 8.81 (1 H, t, *J* 1.5, aryl *H*), 8.71 (2 H, d, *J* 1.5, aryl *H*); *m/z* (APCI+) 329.3 (M⁺). Toluene (100 ml), bis(2-ethylhexylamine) (7.78 ml, 25.9 mmol) and Et₃N (3.61 ml, 25.9 mmol) were added to the reaction flask and the mixture was stirred at room temperature until TLC (CH₂Cl₂–EtOAc 9:1) confirmed completion. After 1 h 30–40 petroleum ether (100 ml) was added. Suction filtration (to remove the Et₃NHCl precipitate) followed by washing with 30–40 petroleum ether (4 \times 50 ml), ensured

complete extraction of the product into the filtrate. The filtrate was evaporated and chromatographed (initially CH₂Cl₂–EtOAc 10:1 as eluent, gradually increasing polarity). Solvent removal and vacuum drying, yielded the product **11** (7.63 g, 99%) as a yellow oil.

***N,N,N,N*-Tetrakis(2-ethylhexyl)-5-trimethylsilylethynyl-isophthalamide (**12**)**

Trimethylsilylacetylene (430 μ l, 3.05 mmol) was added to a mixture of **11** (1.50 g, 2.03 mmol), Pd(OAc)₂ (9.1 mg, 0.04 mmol), PPh₃ (21 mg, 0.08 mmol) and CuI (1.9 mg, 0.01 mol) in Et₃N (8 ml) and the reaction stirred at 50 °C for 1 h. Within 20 min, the mixture had become brown and cloudy. After cooling, the reaction mixture was filtered through silica then chromatographed in chloroform. Solvent removal and vacuum drying yielded the product **12** (1.28 g, 89%) as a yellow oil.

***N,N,N,N*-Tetrakis(2-ethylhexyl)-5-ethynylisophthalamide (**13**)**

K₂CO₃ (1.24 g, 9.00 mmol) was added to a solution of **12** (1.28 g, 1.80 mmol) in THF (40 ml) and MeOH (40 ml). The mixture was stirred at room temperature for 90 min. CH₂Cl₂ (100 ml) was added and the organic layer washed with water (3 \times 40 ml). Chromatography in chloroform followed by vacuum drying yielded **13** as a brown oil (1.082 g, 94%).

5,15-Bis{3,5-bis[*N,N*-bis(2-ethylhexyl)carbamoyl]phenylethynyl}-10,20-bis{(triisopropylsilyl)ethynyl}porphyrinato}Zn(II) (Zn14**)**

A solution of Pd₂(dba)₃ (13.3 mg, 0.0145 mmol), PPh₃ (31.8 mg, 0.121 mmol), and CuI (11.5 mg, 0.0606 mmol) in Et₃N (25 ml) was heated at 70 °C for 30 min under argon. This catalyst solution was then transferred by cannula into an oxygen-free solution of **Zn7** (0.216 g, 0.24 mmol) and aryl acetylene **13** (0.617 g, 0.97 mmol) in toluene (25 ml) and pyridine (500 ml), and the reaction mixture was heated at 80 °C for 4–5 h, with monitoring was by TLC (CH₂Cl₂–4% MeOH) and UV (red shift of Soret band for product). The reaction mixture was then filtered through silica (CH₂Cl₂ as eluent), evaporated and chromatographed in 60–80 petroleum ether–EtOAc–pyridine (10:0.75:0.1) to separate two main green bands. The trace of faster running product was identified as the mono-substituted compound derived from the mono-bromo species and the major, slower running product as the desired compound **Zn14** (0.462 g, 95%).

5,15-Bis{3,5-bis[*N,N*-bis(2-ethylhexyl)carbamoyl]phenylethynyl}-10,20-bis(ethynyl)porphyrinato}Zn(II) (Zn15**)**

TBAF (160 μ l of a 1.0 M solution in THF, 0.160 mmol) was added to **Zn14** (0.160 g, 0.0798 mmol) stirring in CH₂Cl₂ (20 ml). The reaction was complete by TLC (60–80 petroleum ether–EtOAc–pyridine 10:2:0.1) after 15 min, and acetic acid (10 μ l, 0.168 mmol) was added to quench the reaction. The solvents were evaporated and the reaction mixture was chromatographed in 60–80 petroleum ether–EtOAc–pyridine (10:2:0.5). Removal of solvents and vacuum drying yielded the product **Zn15** (0.120 g, 89%) as a green solid.

Polymer (4**)**

To the free acetylene porphyrin **Zn15** (0.223 g, 0.132 mmol) stirring vigorously in a 2 litre flask under dry air at room temperature in CH₂Cl₂ (170 ml) and pyridine (1.7 ml), CuCl (1.04 g, 10.5 mmol) and TMEDA (1.59 ml, 10.5 mmol) were added. The green solution immediately reddened. After 5 min, there was no starting material by TLC (chloroform–1% pyridine), and after 30 min the reaction mixture was washed

repeatedly with water to remove Cu²⁺ salts. The red/brown solution was evaporated and chromatographed (initially chloroform–2% pyridine). The first and major fraction from this column was dissolved in chloroform–1% pyridine (20 ml) and centrifuged (4500 rpm, 10 min), decanted and centrifuged again to remove all insoluble material. The volume was then reduced to ca. 1 ml, polymer precipitated with methanol (20 ml) and centrifuged (4500 rpm, 10 min). The precipitate was resuspended and centrifuged twice with methanol and then three times with 30–40 petroleum ether. Vacuum drying yielded polymer **4** (0.158 g, 71%). Found: C, 76.2; H, 8.7; N, 6.6. [C₁₀₈H₁₅₀N₈O₄Zn]_n requires C, 76.7; H, 8.9; N, 6.6%. λ_{\max} (CHCl₃–1% pyridine)/nm 481 (log ϵ 5.02), 532 (4.96), 698 (4.38), 815 (4.38); ν_{\max} (KBr)/cm⁻¹ 2177 and 2121 (C=C), 1634 (C=O); δ_{H} (500 MHz; CDCl₃, d₅-pyridine) 9.98 (4 H, s, β H), 9.83 (4 H, s, β H), 8.13 (4 H, s, aryl H), 7.45 (2 H, s, aryl H), 3.55 (8 H, br s, NCH₂), 3.36 (8 C, br s, NCH₂), 1.94–0.93 (120 H, m, alkyl H); δ_{C} (125.8 MHz; CDCl₃, d₅-pyridine) 171.06, 153.24, 152.21, 138.47, 132.18, 131.00 (8 C, β C), 125.58, 124.92, 103.20, 102.28, 95.58, 93.87, 87.70, 82.80, 52.80 + 47.02 (CH₂), 37.65 + 36.74 (CH), 30.84 + 30.52 (CH₂), 28.78 (CH₂), 24.16 + 23.76 (CH₂), 23.25 + 23.13 (CH₂), 14.25 + 14.20 (CH₃), 11.01 + 10.84 (CH₃); *m/z* (MALDI) 5097 (trimer M⁺, calc. 5071), 6824 (tetramer M⁺, calc. 6761), 8533 (pentamer M⁺, calc. 8451), 10236 (hexamer M⁺, calc. 10141), 11940 (heptamer M⁺, calc. 11831), 13600 (octamer M⁺, calc. 13520), 15285 (nonamer M⁺, calc. 15210), 17005 (decamer M⁺, calc. 16900), 18732 (11-mer M⁺, calc. 18590), 20375 (12-mer M⁺, calc. 20280), 22048 (13-mer M⁺, calc. 21969); GPC (THF) *M_n* = 53 000; *M_w* = 119 000.

***meso-meso*'-5,15-Bis{3,5-bis[*N,N*-bis(2-ethylhexyl)carbamoyl]phenylethynyl}-10-[(triisopropylsilyl)ethynyl]porphyrinato}-Zn(II) dimer (**Zn₂17**)**

To the mono-protected acetylene porphyrin **Zn16** (0.128 g, 0.0694 mmol) stirring vigorously in a 1 litre flask under dry air at room temperature in CH₂Cl₂ (160 ml) and pyridine (1.6 ml), CuCl (0.550 g, 5.55 mmol) and TMEDA (0.838 ml, 5.55 mmol) were added. The green solution immediately reddened. The reaction was monitored by TLC (chloroform–1% pyridine), and after 15 min no more starting material was seen and the reaction mixture was washed repeatedly with water to remove Cu²⁺ salts. The organic layer was separated and solvents removed. Recrystallisation from CH₂Cl₂ and methanol yielded dimer **Zn₂17** (0.112 g, 87%) as a sticky green solid which hardened on vacuum drying.

Acknowledgements

We are grateful to the EPSRC for supporting this work, and to the EPSRC mass spectrometry service (Swansea) for FAB mass spectra.

References

- 1 W. J. Feast, J. Tsiboukalis, K. L. Pouwer, L. Groenendaal and E. W. Meijer, *Polymer*, 1996, **37**, 5017 *Conjugated Polymers*, eds. J. L. Brédas and R. Silbey, Kluwer Academic, Dordrecht, 1991.
- 2 H. L. Anderson, *Chem. Commun.*, 1999, 2323Z. Bao and L. Yu, *Trends Polym. Sci.*, 1995, **3**, 159.
- 3 S. V. Kershaw, in *Optoelectronic Properties of Inorganic Compounds*, ed. D. M. Roundhill and J. P. Fackler, Plenum, New York, 1999, ch. 10T. Kobayashi, *Nonlinear Opt.*, 1991, **1**, 91.
- 4 C. W. Spangler, *J. Mater. Chem.*, 1999, **9**, 2013L. W. Tutt and T. F. Boggess, *Prog. Quantum Electron.*, 1993, **17**, 299.
- 5 H. S. Nalwa, *Adv. Mater.*, 1993, **5**, 341T. Kaino and S. Tomaru, *Adv. Mater.*, 1993, **5**, 172.
- 6 B. Jiang, S.-W. Yang, D. C. Barbini and W. E. Jones, *Chem. Commun.*, 1998, 213.
- 7 M. J. Therien and S. G. DiMagno, *US Patent*, 1994, 5 371 199.
- 8 A. S. Hay, *J. Org. Chem.*, 1960, **25**, 1275P. Siemsen,

- R. C. Livingston and F. Diederich, *Angew. Chem., Int. Ed.*, 2000, **39**, 2632.
- 9 M. Kijima, I. Kinoshita, T. Hattori and H. Shirakawa, *Synth. Met.*, 1999, **100**, 61T. X. Neenan, M. R. Callstrom, L. M. Scarmoutzos, K. R. Stewart and G. M. Whitesides, *Macromolecules*, 1988, **21**, 3525D. R. Rutherford, J. K. Stille, C. M. Elliott and V. R. Reichert, *Macromolecules*, 1992, **25**, 2294.
 - 10 H. L. Anderson, S. J. Martin and D. D. C. Bradley, *Angew. Chem., Int. Ed. Engl.*, 1994, **33**, 655.
 - 11 S. M. Kuebler, R. G. Denning and H. L. Anderson, *J. Am. Chem. Soc.*, 2000, **122**, 339J. R. G. Thorne, S. M. Kuebler, R. G. Denning, I. M. Blake, P. N. Taylor and H. L. Anderson, *Chem. Phys.*, 1999, **248**, 181.
 - 12 G. S. Wilson and H. L. Anderson, *Chem. Commun.*, 1999, 1539.
 - 13 Q. M. Wang and D. W. Bruce, *Synlett*, 1995, 1267.
 - 14 P. S. Clezy and G. A. Smythe, *Aust. J. Chem.*, 1969, **22**, 239R. Chong, P. S. Clezy, A. J. Liepa and A. W. Nichol, *Aust. J. Chem.*, 1969, **22**, 229J. A. de Groot, R. van der Steen, R. Fokkens and J. Lugtenburg, *Recl. Trav. Chim. Pays-Bas*, 1982, **101**, 35.
 - 15 B. J. Littler, M. A. Miller, C.-H. Hung, R. W. Wagner, D. F. O'Shea, P. D. Boyle and J. S. Lindsey, *J. Org. Chem.*, 1999, **64**, 1391.
 - 16 T. Lange, J. D. van Loon, R. R. Tykwinski, M. Sreiber and F. Diederich, *Synthesis*, 1996, 537.
 - 17 H. L. Anderson, *Tetrahedron Lett.*, 1992, **33**, 1101.
 - 18 R. Schlözer and J.-H. Fuhrhop, *Angew. Chem., Int. Ed. Engl.*, 1975, **14**, 363.
 - 19 R. W. Wagner, T. E. Johnson, F. Li and J. S. Lindsey, *J. Org. Chem.*, 1995, **60**, 5266.
 - 20 V. S.-Y. Lin, S. G. DiMagno and M. J. Therien, *Science*, 1994, **264**, 1105V. S.-Y. Lin and M. J. Therien, *Chem. Eur. J.*, 1995, **1**, 645.
 - 21 For other recent references to Heck–Sonogoshira coupling of meso-halo porphyrins see: S. Shanmugathan, C. K. Johnson, C. Edwards, E. K. Matthews, D. Dolphin and R. W. Boyle, *J. Porphyrins Phthalocyanines*, 2000, **4**, 228D. A. Schulz, H. Lee, R. K. Kumar and K. P. Gwaltney, *J. Org. Chem.*, 1999, **64**, 9124D. A. Schulz, K. P. Gwaltney and H. Lee, *J. Org. Chem.*, 1998, **63**, 4034D. P. Arnold, R. C. Bott, H. Eldridge, F. M. Elms, G. Smith and M. Zojaji, *Aust. J. Chem.*, 1997, **50**, 495S. M. LeCours, H.-W. Guan, S. G. DiMagno, C. H. Wang and M. J. Therien, *J. Am. Chem. Soc.*, 1996, **118**, 1497R. W. Boyle, C. K. Johnson and D. Dolphin, *J. Chem. Soc., Chem. Commun.*, 1995, 527.
 - 22 F. Diederich, in *Modern Acetylene Chemistry*, ed. P. J. Stang and F. Diederich, ch. 13, VCH, Weinheim, 1995.
 - 23 A. Kraft, *Liebigs Ann. Chem.*, 1997, 1463.
 - 24 J. C. Nelson, J. K. Young and J. S. Moore, *J. Org. Chem.*, 1996, **61**, 8160.
 - 25 O. M. Gelsen, D. D. C. Bradley, H. Murata, N. Takada, T. Tsutsui and S. Saito, *J. Appl. Phys.*, 1992, **71**, 1064.
 - 26 S. D. Phillips, R. Worland, G. Yu, T. Hagler, R. Freedman, Y. Cao, V. Yoon, J. Chiang, W. C. Walker and A. J. Heeger, *Phys. Rev. B: Condens. Matter*, 1989, **40**, 9751.
 - 27 T. Hasegawa, K. Ishikawa, T. Koda, K. Takeda, H. Kobayashi and K. Kubodera, *Synth. Met.*, 1991, **43**, 3151.
 - 28 For an introduction to the z-scan technique see: M. Sheik-Bahae, A. A. Said, T.-H. Wei, D. J. Hagan and E. W. Van Stryland, *IEEE J. Quantum Electron.*, 1990, **26**, 760. We have previously reported z-scan measurements on **2** at 532 nm: F. M. Qureshi, S. J. Martin, X. Long, D. D. C. Bradley, F. Z. Henari, W. J. Blau, E. C. Smith, C. H. Wang, A. K. Kar and H. L. Anderson, *Chem. Phys.*, 1998, **231**, 87. For reports of z-scan measurements on other porphyrins see: F. Z. Henari, W. J. Blau, L. R. Milgrom, G. Yahiolglu, D. Phillips and J. A. Lacey, *Chem. Phys. Lett.*, 1997, **267**, 229; K. Kandasamy, S. J. Shetty, P. N. Puntambekar, T. S. Srivastava, T. Kundu and B. P. Singh, *Chem. Commun.*, 1997, 1159; K. Kandasamy, K. D. Roa, R. Deshpande, P. N. Puntambekar, B. P. Singh, S. J. Shetty and T. S. Srivastava, *Appl. Phys. B*, 1997, **64**, 479; M. Terazima, H. Shgimizu and A. Osuka, *J. Appl. Phys.*, 1997, **81**, 2946; A. G. Bezerra, I. E. Borissevitch, R. E. de Araujo, A. S. L. Gomes and C. B. de Araujo, *Chem. Phys. Lett.*, 2000, **318**, 511.
 - 29 P. B. Chapple, J. Staromlynska, J. A. Hermann, T. J. McKay and R. G. McDuff, *J. Nonlinear Opt. Phys. Mater.*, 1997, **6**, 251.
 - 30 P. N. Butcher and D. Cotter, *The Elements of Nonlinear Optics*, 1990, Cambridge University Press.
 - 31 A. Mathy, K. Ueberhofen, R. Schenk, H. Gregorius, R. Garay, K. Müllen and C. Bubeck, *Phys. Rev. B*, 1996, **53**, 4367.
 - 32 R. G. Ispasoiu and T. Goodson, *Opt. Commun.*, 2000, **178**, 371.